Fracture Criteria for Piezoelectric Ceramics

Leslie Banks-Sills

School of Mechanical Engineering, Tel Aviv University, Ramat Aviv, 69978, Israel
Division of Solid Mechanics, Lund University, Lund SE-221 00, Sweden
banks@eng.tau.ac.il

Abstract An analytical, numerical and experimental investigation was carried out to determine fracture criteria for piezoceramics with poling parallel and perpendicular to the crack faces. The asymptotic expressions of stress, strain, electric flux density and electric fields were derived. For a piezoelectric material, in addition to the usual three modes of fracture, there is a fourth mode associated with the electric field. The asymptotic expressions were used for determining the energy release rate and extending a conservative interaction energy or *M*-integral for calculating the intensity factors associated with piezoelectric material for energetically consistent boundary conditions on the crack faces. Tests were performed on four-point bend PZT-5H fracture specimens with the poling direction parallel to the crack faces. The specimens were analyzed numerically by means of the finite element method. Finally, a mixed mode fracture criterion for piezoelectric ceramics was developed. This criterion is based upon the energy release rate and two phase angles, determined from the ratio between the intensity factors K_{IV} and K_I, for the first, and K_{II} and K_I, for the second. This data and that taken from another source for poling perpendicular to the crack faces were used to produce failure criteria for each case.

Keywords Conservation integrals, Four-point bend tests, Mixed mode fracture, Piezoelectric ceramics

1. Introduction

Piezoelectric ceramics are in widespread use as sensors and actuators in smart structures, despite the absence of a fundamental understanding of their fracture behavior. Piezoceramics are brittle and susceptible to cracking. As a result of the importance of the reliability of these devices, there has been tremendous interest in studying the fracture and failure behavior of such materials. To understand failure mechanisms of piezoelectric materials and maintain the stability of cracked piezoelectric structures operating in an environment of combined electromechanical loading, analysis of the mechanical and electrical behavior is a prerequisite.

There have been many fracture tests carried out on piezoelectric material [1–12]. Fracture criteria have been presented in [10-17]. Each of these is based on the energy release rate. In fact, in [17] the energy was separated into its mechanical and electrical parts. Assuming impermeable crack face conditions, it was concluded in [17] that crack propagation of poled piezoelectric material is governed by the mechanical energy release rate. However, crack growth driven by purely electric fields in poled ferroelectrics has been observed in experiments [18,19]. A local energy release rate criterion was presented in [14] and [15] based on electric nonlinearity caused by a domain switching zone ahead of the crack tip. Impermeable crack face boundary conditions were also assumed there. The energy release rate obtained in [13] was used in [10] as a fracture criterion for analyzing results obtained with four-point bend specimens. This expression is based upon the load and electric current measured during the experiment. For an applied field of 0.5 MV/m, the energy release rate was zero or negative, which is not physically reasonable. Fracture curves of K_I versus K_{IV} were presented in [16] using impermeable and permeable assumptions. For both

conditions, there were discrepancies between the measured and calculated curves. A recent review article may be found in [20].

2. Fracture Criteria

A generalized fracture criterion for piezoelectric ceramics requires the development of a unified theory, which consists of mixed mode behavior, together with application of the energetically consistent crack face boundary conditions. In [11], the derivation for the energy release rate begins with the expression [21]

$$\mathcal{G} = \frac{1}{2}\boldsymbol{k}^T \boldsymbol{L}^{-1}\boldsymbol{k} \tag{1}$$

where $\boldsymbol{k}$ is the intensity factor vector given by

$$\boldsymbol{k}^T = \left[K_{II}, K_I, K_{III}, K_{IV}\right] \tag{2}$$

and the superscript T represents transpose. In Eq. (1), the 4×4 matrix $\boldsymbol{L}$ is one of the Barnett-Lothe tensors whose components are related to material properties.

For the numerical calculations, the intensity factors were normalized so that

$$\hat{\boldsymbol{k}} = \boldsymbol{V}^{-1}\boldsymbol{k} \tag{3}$$

where

$$\boldsymbol{V} = \begin{bmatrix} E_A\sqrt{L} & 0 & 0 & 0 \\ 0 & E_A\sqrt{L} & 0 & 0 \\ 0 & 0 & G_T\sqrt{L} & 0 \\ 0 & 0 & 0 & e_{26}\sqrt{L} \end{bmatrix} \tag{4}$$

E_A is Young's modulus in the poling direction, G_T is the shear modulus perpendicular to the poling direction, e_{26} is a contracted piezoelectric constant and L is a geometrical length parameter. The Barnett-Lothe tensor $\boldsymbol{L}^{-1}$ is normalized as

$$\hat{\boldsymbol{L}}^{-1} = \boldsymbol{V}\boldsymbol{L}^{-1}\boldsymbol{V}. \tag{5}$$

In this way, the diagonal and off-diagonal elements of $\boldsymbol{L}^{-1}$ are the same order of magnitude contributing to the accuracy of the intensity factor calculation [22]. Note that the units of $\boldsymbol{L}^{-1}$ are N/m.

The criterion presented in [11] with mode III deformation omitted is given by

$$\mathcal{G}_c = \mathcal{G}_{Ic}\left(1 + 2a_1\tan\psi + 2a_2\tan\phi + 2a_3\tan\psi\tan\phi + a_4\tan^2\psi + a_5\tan^2\phi\right) \tag{6}$$

where

$$a_1 = \frac{\hat{L}_{24}^{-1}}{\hat{L}_{22}^{-1}}, \quad a_2 = \frac{\hat{L}_{12}^{-1}}{\hat{L}_{22}^{-1}}, \quad a_3 = \frac{\hat{L}_{14}^{-1}}{\hat{L}_{22}^{-1}}, \quad a_4 = \frac{\hat{L}_{44}^{-1}}{\hat{L}_{22}^{-1}}, \quad a_5 = \frac{\hat{L}_{11}^{-1}}{\hat{L}_{22}^{-1}} \tag{7}$$

and

$$\mathcal{G}_{Ic} = \frac{1}{2}\hat{L}_{22}^{-1}\hat{K}_{Ic}^2. \tag{8}$$

To obtain $\mathcal{G}_{Ic}$, values of $\mathcal{G}_I$ given by

$$\mathcal{G}_I = \frac{1}{2}\hat{L}_{22}^{-1}\hat{K}_I^2 \tag{9}$$

are obtained at failure for each test and averaged. In Eq. (7), the parameters $\hat{L}_{ij}^{-1}$ $(i, j = 1,...,4)$ are found from Eq. (5). The phase angles are defined as

$$\psi = \tan^{-1}\frac{\hat{K}_{IV}}{\hat{K}_I}, \qquad \phi = \tan^{-1}\frac{\hat{K}_{II}}{\hat{K}_I}. \tag{10}$$

Eq. (6) represents a three-dimensional failure surface for the case in which the crack faces are at an angle to the poling direction (which is in the plane) and in which the critical energy release rate $\mathcal{G}_c$ is a function of the phase angles ψ and ϕ. There is an assumption that the crack propagates in a self-similar manner.

Tests were carried out in [10] on four-point bend specimens fabricated from the piezoelectric ceramic PIC-151. This material is similar to PZT-5H. In these experiments, the crack faces were perpendicular to the poling direction and both mechanical loads and electric fields were applied. The electric field was perpendicular to the crack faces. Those experimental results were analyzed in [11]. In the analyses, $\hat{K}_{II}$ was found to be zero implying that ϕ in Eq. $(10)_2$ is zero. Hence, Eq. (6) may be rewritten as

$$\mathcal{G}_c = \mathcal{G}_{Ic}\left(1 + 2a_1 \tan\psi + a_4 \tan^2\psi\right). \tag{11}$$

The experimental results and the failure curve of Eq. (10), shown as the solid line, are presented in Fig. 1. Note that a is crack length. The value of $\mathcal{G}_{Ic}$ was found as 8.6 N/m. There is good agreement between the experimental data and the failure curve. To this end, the root mean square error (RMSE) given by

$$\text{RMSE} = \sqrt{\frac{\sum_{\text{N}}\left(\mathcal{G}_c^{\text{experiment}} - \mathcal{G}_c^{\text{theoretical}}\right)^2}{N}} \tag{12}$$

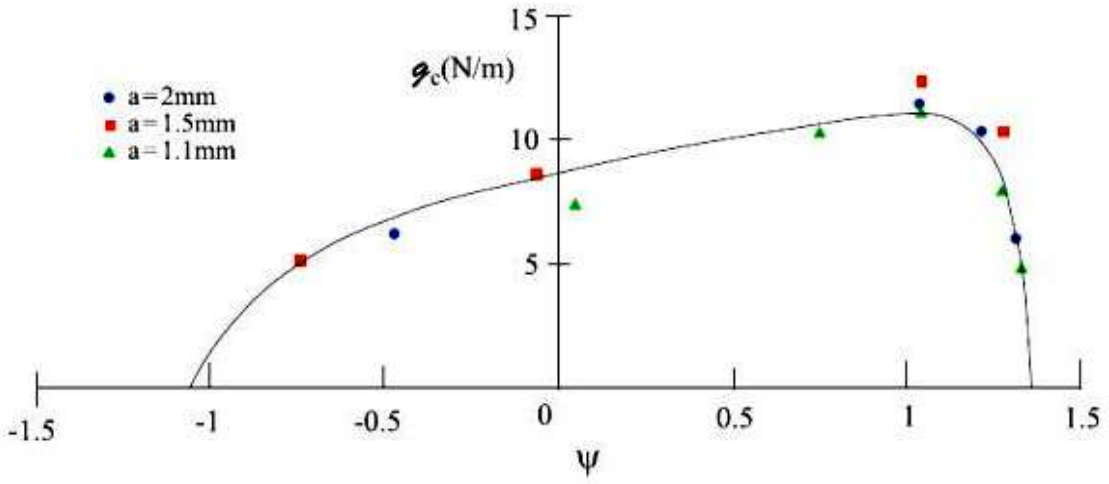

Figure 1. Failure curve and experimental results (PIC-151) [10] obtained in [11]. The crack is perpendicular to the poling direction.

was calculated to be 0.89 N/m. In Eq. (12), $\mathcal{G}_c^{\text{experiment}}$ is the experimental value or the point plotted in Fig. 1, $\mathcal{G}_c^{\text{theoretical}}$ is the value on the curve of $\mathcal{G}_c$ for the experimental value of ψ as calculated from Eq. (11) and N is the number of tests.

As a result of the coupling between the first and fourth modes of fracture, which is expressed by the second term in parentheses of the right hand side of Eq. (11), the fracture curve in Fig. 1 is not symmetric with respect to $\psi = 0$. Furthermore, it should be emphasized that the apparent fracture toughness $\mathcal{G}_{Ic}$ should not be used to predict catastrophic failure. Only the mixed mode fracture curve presented in Eq. (11) and Fig. 1 should be used to predict failure. To interpret the failure curve for a structure fabricated from the same material and containing a crack perpendicular to the poling direction, values of $\mathcal{G}_c$ below the curve are considered safe; for those above it, failure may be expected. Of course, a probabilistic analysis should be carried out.

Next, a fracture criterion for tests carried out in [12] on four-point bend specimens fabricated from PZT-5H (Morgan Electro Ceramics, Wrexham, UK) with poling parallel to the crack faces is presented. In that study, modes I, II and IV were present. Since poling is parallel to the crack faces, $a_1 = a_2 = 0$ in Eq. (7). Hence, the fracture criterion in Eq. (6) becomes

$$\mathcal{G}_c = \mathcal{G}_{Ic}\left(1 + 2a_3 \tan\psi \tan\phi + a_4 \tan^2\psi + a_5 \tan^2\phi\right). \tag{13}$$

Note that during the tests, the electric field was applied perpendicular to the crack faces. The value of $\mathcal{G}_{Ic}$ was found to be 20.3 N/m. In Fig. 2, the three-dimensional failure surface in Eq. (13) is plotted. The points shown are the experimental values obtained by analyzing the results from the four-point bend tests.

In order to have a better view of the scatter, the phase angle ϕ in the criterion of Eq. (13) was assumed zero resulting in

$$\mathcal{G}_c = \mathcal{G}_{Ic}\left(1 + a_4 \tan^2\psi\right). \tag{14}$$

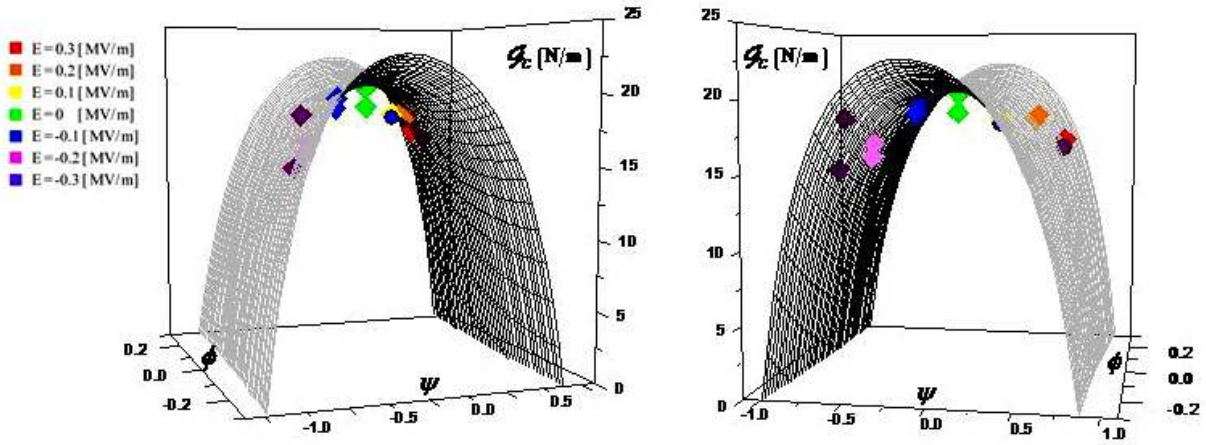

Figure 2. Two views of the three-dimensional failure surface from Eq. (13) with the test data shown. The crack is parallel to the poling direction.

This curve is plotted with $\mathcal{G}_{Ic} = 20.3$ N/m in Fig. 3. The test values $\mathcal{G}_c$, recalculated with $\hat{K}_{II} = 0$, together with the values of ψ are plotted as points in Fig. 3. This may be justified since the values of $\hat{K}_{II}$ are small with respect to $\hat{K}_I$ and $\hat{K}_{IV}$ except for one specimen. The root mean square error in Eq. (12) was calculated as 1.10 N/m for the three-dimensional surface and 1.05 N/m for the two-dimensional curve.

Finally, the crack propagation angle θ measured from a line extending ahead of the crack was obtained for each test. The angle varied between 1^0 and 10^0. Points for $9^0 \le \theta \le 10^0$ showed the greatest scatter from the theoretical curve, although even for 5^0 and 6.5^0 there was some scatter. Generally, smaller propagation angles led to less scatter in the test results as compared to the theoretical curve. There seemed to be no apparent correlation between large values of $\hat{K}_{II}$ or

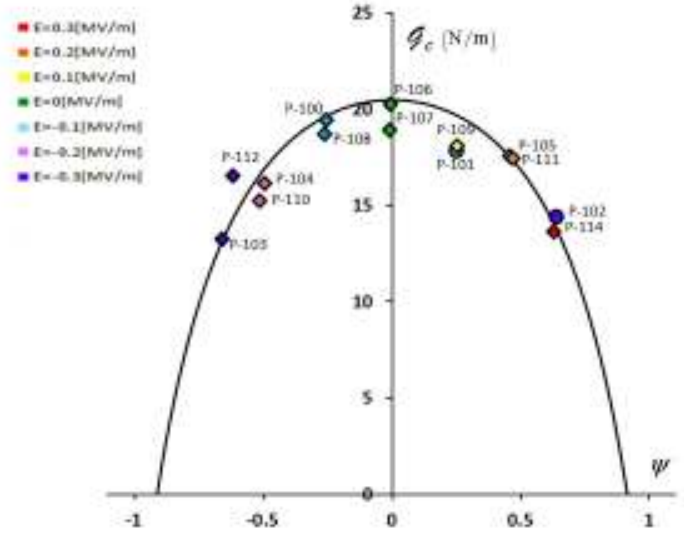

Figure 3. Two-dimensional failure curve from Eq. (14) with test data shown. The crack is parallel to the poling direction.

$\hat{K}_{IV}$ and θ. Theoretically, larger values of $\hat{K}_{II}$ imply larger values of θ. Recall that the fracture criteria were developed for self-similar crack propagation. For these small propagation angles, the results appear to be acceptable. But if one has a substantial value for θ, the criteria presented here may not be used.

Acknowledgements

I would like to acknowledge the contributions of Dr. Yael Motola, Ms. Liat Heller, Dr. Victor Fourman and Mr. Rami Eliasi in carrying out tests and analyses described here.

References

[1] A.G. Tobin, Y.E. Pak, Effect of electric fields on fracture behavior of PZT ceramics. SPIE, 1916 (1993) 78–86.
[2] S. Park, C.T. Sun, Fracture criteria for piezoelectric ceramics. J Am Cer Soc, 78 (1995) 1475–1480.
[3] H. Wang, R.N. Singh, Crack propagation in piezoelectric ceramics: effects of applied electric field. J Appl Phys, 81 (1997) 7471–7479.
[4] C.S. Lynch, Fracture of ferroelectric and relaxor electro-ceramics: influence of electric field. Acta Mater, 46 (1998) 599–608.
[5] R. Fu, T-Y. Zhang, Effects of an electric field on the fracture toughness of poled lead zirconate titanate ceramics. J Am Cer Soc, 83 (2000) 1215–1218.
[6] Y. Shindo, M. Oka, K. Horiguchi, Analysis and testing of indentation fracture behavior of piezoelectric ceramics under an electric field. J Engng Mater Techno, 123 (2001) 293–300.
[7] Y. Shindo, F. Narita, M. Mikami, Double torsion testing and finite element analysis for determining the electric fracture properties of piezoelectric ceramics. J Appl Phys, 97 (2005) 114109-1–114109-7.
[8] G.A. Schneider, F. Felten, R.M. McMeeking, The electrical potential difference across cracks in PZT measured by Kelvin Probe Microscopy and the implications for fracture. Acta Mater, 51 (2003) 2235–2241.
[9] X.P. Zhang, S. Galea, L. Ye, Y.W. Mai, Characterization of the effects of applied electric fields on fracture toughness and cyclic electric field induced fatigue crack growth for piezoceramic PIC 151. Smart Mater Struc, 13 (2004) 9–16.
[10] H. Jelitto, H. Kessler, G.A. Schneider, H. Balke, Fracture behavior of poled piezoelectric PZT under mechanical and electrical loads. J Euro Cer Soc, 25 (2005) 749–757.
[11] Y. Motola, L. Banks-Sills, V. Fourman, On fracture testing of piezoelectric ceramics. Int J Fract, 159 (2009) 167–190.
[12] L. Banks-Sills, L. Heller, V. Fourman, A supplementary study on fracture tests of piezoelectric material: cracks parallel to the poling direction. Int J Fract, 175 (2012) 109–125.
[13] Z. Suo, Mechanics concepts for failure in ferroelectric ceramics, in: A.V. Srinivasan (Ed.), Smart Structures and Materials, AMD 123, American Society of Mechanical Engineers, New York, 1991, pp. 1–6.
[14] H. Gao, T-Y. Zhang, P. Tong, Local and global energy release rates for an electrically yielded crack in a piezoelectric ceramic. J Mech Phys Solids, 45 (1997) 491–510.
[15] C.C. Fulton, H. Gao, Effect of local polarization switching on piezoelectric fracture. J Mech Phys Solids, 49 (2001) 927–952.
[16] H. Jellito, F. Felten, C. Hausler, H. Kessler, H. Balke, G.A. Schneider, Measurment of energy release rates for cracks in PZT under electromechanical loads. J Euro Cer Soc, 25 (2005) 2817–2820.
[17] S. Park, C.T. Sun, Effect of electric field on fracture of piezoelectric ceramics. Int J Fract, 70 (1995) 203–216.

[18] H. Cao, A.G. Evans, Electric-field-induced fatigue crack growth in piezoelectrics. J Am Cer Soc, 77 (1994) 1783–1786.
[19] J.K. Shang, X. Tan, A maximum strain criterion for electric-field-induced fatigue crack propagation in ferroelectric ceramics. Mater Sci Engng A, 301 (2001) 131–139.
[20] M. Kuna, Fracture mechanics of piezoelectric material–where are we right now? Eng Fract Mech, 77 (2010) 309–326.
[21] Z. Suo, C.M. Kuo, D.M. Barnett, J.R. Willis, Fracture mechanics for piezoelectric ceramics. J Mech Phys Solids, 40 (1992) 739–765.
[22] L. Banks-Sills, Y. Motola, L. Shemesh, The *M*-integral for calculating intensity factors of an impermeable crack in a piezoelectric material. Engng Fract Mech, 75 (2008) 901–925.